Entry to the Stockholm Junior Water Prize 2019

A Novel Approach for Purifying Contaminated Drinking Water using Carbon Aerogel Electrodes Synthesized from Thermoplastic Waste

Authors;

Didarul Islam*****

Md. Shahriar Hasan

Bangladesh

I. ABSTRACT

The major emphasis of this study was to develop a rapid, portable and highly-effective water purification device for on-spot water remediation with minimal energy consumption in a single design. Capacitive deionization (CDI) is an emerging and promising technique for addressing this goal and thus carbon aerogels (CAs) was synthesized from thermoplastic waste as a potential electrode material for fabricating CDI electrode. A non-invasive, straightforward and chemical-free strategy was developed to synthesize CAs by overcoming the fundamental synthesizing route drawbacks of the typical sol-gel method. In addition, CAs were immobilized on a locally available, biocompatible and flexible jute thread substrate in a simple and scalable pathway for an effective electrode-water interface. The single-pass filtration experiments conducted at 1.2 V through the gravitational force demonstrated that the electrode fabricated from PET carbon aerogels is superiorly efficient by eliminating approximately 100% of both NaCl and As ($^{5+}$) contaminants ions across a wide range of feedstock concentrations (50-1000 ppm) due to the rapid formation of the electrical double layer. Additionally, the electrode fabricated from mixed plastic carbon aerogels exhibits overall high filtration efficiency of 93.53% at the intermediate concentration range of $\leq$1000 ppm, where the commercial reverse osmosis system was proven relatively ineffective. This interdisciplinary study opens numerous possibilities for generating potable and affordable water using rapid, miniaturized and versatile devices during natural disasters or other emergency situations when the access to electrical power is inadequate with protecting the ecosystem from the consequences of thermoplastic debris problem.

II. TABLE OF CONTENTS

III. KEYWORDS

Thermoplastic, carbon aerogel, capacitive deionization, sol-gel method, salinity, arsenic.

IV. ABBREVIATIONS AND ACRONYMS

CAs: Carbon aerogels	**CDI:** Capacitive deionization
PET: Polyethylene terephthalate	**PS:** Polystyrene
HDPE: High-density polyethylene	**HTC:** Hydrothermal carbonization
CMC: Sodium carboxymethyl cellulose	**DIW:** Deionized water
PCA: PET carbon aerogels	**MCA:** Mixed plastic carbon aerogels
AEM: Active electrode material	**RO:** Reverse osmosis

V. ACKNOWLEDGEMENTS

We would like to sincerely thank the authority of Bangladesh Council of Scientific and Industrial Research (BCSIR) and Bangladesh Atomic Energy Commission for providing the research and laboratory facilities. We would also like to acknowledge Dr. Md. Abdul Gafur from Pilot Plant and Process Development Centre of BCSIR for his valuable supervision in the characterization and experimental stages. We are also grateful to Dr. Tanvir Ahmed of the Department of Civil Engineering at Bangladesh University of Engineering and Technology for his dedication and expertise during the research.

VI. BIOGRAPHY

Didarul Islam is an 11th-grade student at Kushtia Government College. He is an optimistic and fearlessly curious about the fascinating arena of nanophysics and material science. In his pastime, he loves practicing extemporaneous debating and playing the harmonica. However, he has been working for the past three years to envisaged a nanotechnology-based energy efficient device for sustainable water treatment and founded a social enterprise to implement the idea. He wants to continue his research in the field of environmental engineering and material science in order to develop a novel solution to tackling the global water crisis.

Md. Shahriar Hasan is in his senior year at Dhaka College, Dhaka. He had reflected his enthusiasm in environmental science, computer vision and machine learning. He also researched in disease prediction, machine failure prediction and natural superabsorbent polymers. Recently, he has grown his passion in nanoscience and nanotechnology. In the future, Shahriar hopes to conduct research in the field of nanotechnology and artificial intelligence to create novel and automated solutions to solve the social and environmental problems faced around the world.

1. INTRODUCTION

1.1. Significance of Study

Access to safe and abundant water is the fundamental demand for humankind, but nowadays the quality of potable water resources is tremendously threatened by salinity or poisonous contaminants like arsenic. More than 105.6 million hectares of area in Bangladesh that is highly affected by the salinity problem and large numbers of pregnant women and children in the coastal areas are being diagnosed with pre-eclampsia, eclampsia, and hypertension due to the increased salinity of drinking water (Rabbani, Munira, & Saif, 2018). In addition, Bangladesh is currently facing a serious threat to public health, with 85 million people at risk for arsenic contamination in groundwater and in food crops (M.F.Hossain, 2019). In Bangladesh, an estimated 97% of the rural population is dependent on groundwater sources for drinking and household purposes but nowadays the groundwater contamination has reached alarming proportions due to the devastating effect of climate change (Jahan, 2016) which is one of the major challenges to achieving the Sustainable Development Goal (SDG) of 6.1. Typically, the concentration of both saline (mainly NaCl) and the arsenic contaminated solution has not been found to exceed 1000 ppm in countrywide groundwater aquifers (Jahan, 2016) thus there is significant technological and social importance to develop a water purification approach for the contaminated concentration range of ≤1000 ppm. The main challenge with conventional technologies is that they require a tremendous amount of energy, expensive and troublesome membranes, high-pressure pump with labour and maintenance intensive and the combination of highly efficient and rapid deionization or heavy metal cleanup is particularly challenging to achieve (Moronshing & Subramaniam, 2017).

Capacitive deionization (CDI) is an emerging and promising approach to address the limitations of conventional technologies as a rapid, energy efficient, and environmentally friendly water treatment process (Fan, Tseng, Li, & Hou, 2016). Fundamentally, CDI is based on the electrosorption of ions that transfers ions from aqueous solutions to a porous carbon electrode surface by imposing an external electric field on a pair of electrodes (Kim, Gorski, & Logan, 2017). The positively and negatively charged ions are then electrostatically adsorbed via electrostatic interactions and an electrical double layer (EDL) is formed at the electrode surface which is acts as a similar to supercapacitor (Kim, Gorski, & Logan, 2017; Farmer, Richardson, Fix, Thomson, & May, 1996). Electrodes are regenerated by electrical discharge or removing the applied electric potential to release the captured ions back to a concentrated flow (Gao, Omosebi, Landon, & Liu, 2015). The viability of this technique demands

electrode materials that are highly effective in a low operating electric potential and hydrophobic nano carbons are needed to immobilize on an optimal substrate to increase mechanical robustness and hydrophilicity for an electrode-water interface for effective desalination and heavy metal cleanup.

In recent decades, the area of carbon aerogels (CAs) research has been extensively investigated for electrochemical double layer capacitors and electrosorptive processes including CDI and attracted intensive attention of researchers and industrialists due to its monolithic structure, high electrical conductivity, high specific surface area, and controllable pore size distribution (Xu, Drewes, Heil, & Wang, 2008; Jia & Zhang, 2016). Aerogels are ultralight mesoporous foams with an interconnected network of nanometer-sized particles, that can combine multiple extreme physical and chemical properties in a single solid material (Karaaslan, Kadla, & Ko, 2016). However, CAs are highly porous amorphous carbon materials in a three-dimensional interconnected framework of carbon nanoparticles with extremely low density and ultrafine, open pore structure (Karaaslan, Kadla, & Ko, 2016; Bi, et al., 2013). The interconnected carbonaceous framework endows CAs with excellent electrical properties, mechanical robustness, ultra-high temperature resistance, low mass density, chemical stability and high specific surface area (Hu, Tan, & Long, 2016; Zhang, Feng, Jiang, & Feng, 2018).

Typically, CAs were synthesized via the polycondensation of resorcinol ($C_6H_4(OH)_2$) with formaldehyde (CH_2O) in the presence of catalysts either base or acid in a sol-gel method (Zhang, Feng, Jiang, & Feng, 2018). Finally, supercritical drying and pyrolysis at above 1000 °C in an inert atmosphere were performed to obtain CAs through the carbonization of organic gels (Araby, et al., 2016). However, the sol-gel method is tremendously sophisticated, destructive, and impractical for industrial-scale manufacturing of CAs due to the expensive and hazardous precursors, supercritical drying, multiple solvent exchanges and other shortcomings including large volume shrinkage and high-temperature carbonization process (Zhang, Feng, Jiang, & Feng, 2018; Karaaslan, Kadla, & Ko, 2016). In order to solve the drawbacks of the conventional route that restrict further development and applications of CAs, it is urgent to develop a non-invasive, chemical-free and feasible CAs synthesis approach.

However, Bangladesh is suffering from the worst plastic waste problems for the past few years due to its rapidly growing readymade garments and packaging industries (Mahmud, 2018; Molla, 2018). Around 73,000 tonnes of thermoplastic waste including polyethylene (PE), polystyrene (PS) and polyethylene terephthalate (PET) derivatives end up in the sea every day through the rivers and that

creates a serious environmental crisis (Mahmud, 2018). In addition, every year in Bangladesh, more than 4 billion PET ($C_{10}H_8O_4$) bottles are manufactured and most of them are discarded after being used once which produces toxic gases and releases microplastics in the presence of sunlight (Sarker, Kabir, Rashid, Molla, & Mohammad, 2011). Existing solution for PET recycling is producing lightweight carpets and synthetic yarn but still, the method is sophisticated and has low market value.

1.2. Structure of Research & Strategy

This research reveals that the thermoplastic polymer waste has an outstanding potential to synthesize CAs instead of carcinogenic and toxic chemical precursors like resorcinol and formaldehyde due to the presence of long linear or branched chains of hydrocarbon and negligible amounts of mineral impurities of their chemical constitution (Jagdale, Sharon, Kalita, Maldar, & Sharon, 2012). In this study, highly porous CAs was synthesized by three phases, including HTC, freeze-drying and post-pyrolysis process using thermoplastic waste as the raw material. HTC was performed at 180 °C to convert raw thermoplastic into spongy hydrogels, and to eliminate supercritical drying, freeze-drying was performed to obtained thermoplastic aerogel. Subsequently, CAs mesoporous foams having a high surface area were obtained by the final carbonization at 700 °C under an N_2 atmosphere. However, any oxidized toxic carbon compounds like carbon monoxide and dioxane were not produced during the heat treatment of thermoplastic polymer due to the conversion of thermoplastic waste into CAs in the absence of oxygen (Jagdale, Sharon, Kalita, Maldar, & Sharon, 2012).

After the carbonization process, biocompatible and flexible jute thread was utilized as a substrate for immobilizing the CAs and also increasing the mechanical robustness and hydrophilicity. The natural porosity of the high-cellulosic jute thread and its hydrophilicity would symbiotically assist the CAs during CDI and would also be adaptable to a variety of geometries. Instead of conventional nickel foam, jute thread was utilized as an optimal substrate to fabricate electrically conductive CDI electrode due to its biocompatibility, low cost, easy availability and chemical inertness (Herou, Schlee, Jorge, & Titirici, 2018). Due to the formation of an EDL at the electrode-solution interface, the best performance was achieved via electrosorption of Sodium Chloride (NaCl) and Arsenic (As^{5+}) at 1.2 V. Considering the high performance, low energy consumption and locally available cheap raw materials, CAs synthesized from thermoplastic waste have a great potential for rapid deionization of both saline contaminated groundwater or brackish water and heavy metal cleanup without producing pollutants like NO_X, SO_2, and other volatile organic compounds.

2. EXPERIMENTAL SECTION

2.1. Materials & Chemicals

All chemicals were obtained from commercial sources and were analytically pure and used without further purification. Sodium Chloride (NaCl, ACS reagent, ≥ 99.0%), Arsenic Pentoxide (As_2O_5, 99.3% Sigma), Sodium Carboxymethyl Cellulose (($C_6H_7O_2(OH)_2CH_2COONa$, CMC, ≥ 99.1%) and Acetone (($(CH_3)_2CO$, AR, 99.8%) were collected from the local distributor of Sigma Aldrich (Merck KGaA, Germany). Polypropylene bar was acquired from the local grocery shop. Jute thread was obtained from A.R. Jute Mills (Pvt.) Ltd., Kushtia. Copper sheet was supplied by TechshopBD and PS foam, HDPE bag and PET bottles were collected from the near street market.

2.2. Synthesis of CAs from Thermoplastic Waste

First, the PS foam, HDPE bag and plastic bottles (labelled as PET) were crushed into fine pieces to obtain the desired size fractions (3-5 mm) and then washed with DIW for several times to get rid of all the dirt particles. Then 5.0 g of mixed plastic (50 wt.% PS, 25 wt.% HDPE and 25 wt.% PET) or 5.0 g of PET waste was put into Teflon-lined stainless-steel autoclave reactor (SS316) for HTC. The autoclave was heated at 180 °C for 6 h under self-generated pressure in a closed system to produce the spongy thermoplastic hydrogels. Subsequently, the spongy hydrogels were taken out and immersed in hot water (around 60 °C) for 2 days to remove soluble impurities. Then corresponding thermoplastic aerogel were obtained by freeze-drying at -10 °C for 2 h. Finally, the CAs mesoporous foams with the high specific surface area were achieved by placing the mixed plastic aerogel or PET aerogel in an electric muffle furnace for final carbonization at 700 °C for 1 h in N_2 atmosphere. After that, the system was left overnight to cool down automatically and the dark powder was crushed with mortar to get fine particle sized mixed plastic CAs (labelled as MCA) and PET CAs powder (labelled as PCA).

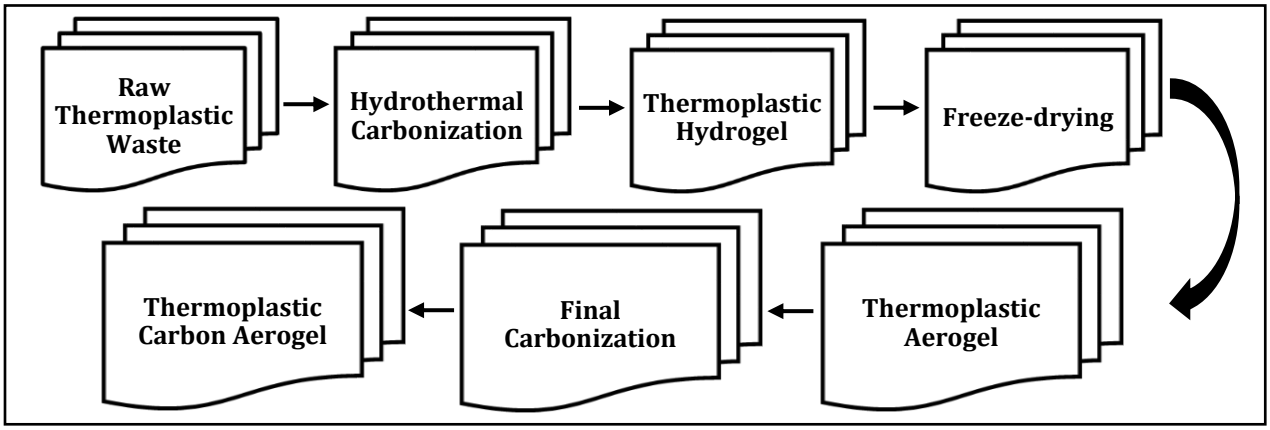

Figure 1: Flowchart illustrating the synthesis of thermoplastic carbon aerogel

2.3. Fabrication of CAs Thread Electrode

Phase 1:

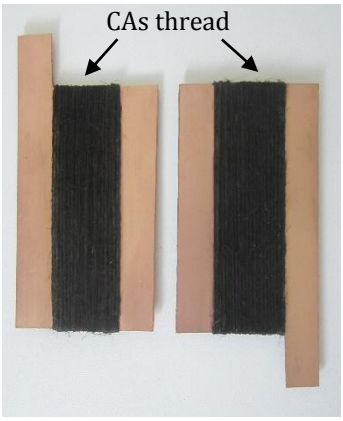

Figure 2: CAs thread on the copper sheet to form the electrode

The CAs thread electrodes were fabricated from both MCA and PCA samples to evaluate their potential as an electrode material for CDI application. For this purpose, the locally obtained pristine jute thread was poured into DIW to soaked for three days and washed with acetone several times to remove non-cellulosic impurities and waxy substances. In order to uniformly disperse CAs in an aqueous solution, 2.5 g of CMC powder as a cellulose derivative non-toxic surfactant was dissolved in 50 ml of DIW and stirred for 1 h. Subsequently, 5.0 g of MCA or PCA powder was dispersed in 50 mL of CMC solution, followed by a 20 min probe sonication. After that, 10 g of jute thread was dip coated in the 25 ml of uniform dispersion of CAs, dried in an oven at 80 °C for 1 h, washed with ultra-pure DIW to remove soluble impurities from the outermost surface and re-dried at 60 °C for 3 h to form the CAs thread. Instead of expensive typical titanium alloy, the CAs thread was strongly and closely winded across a flat copper sheet (5.0 Inch × 2.5 Inch) where the copper sheet serves both as a current collector and structural support.

Phase 2:

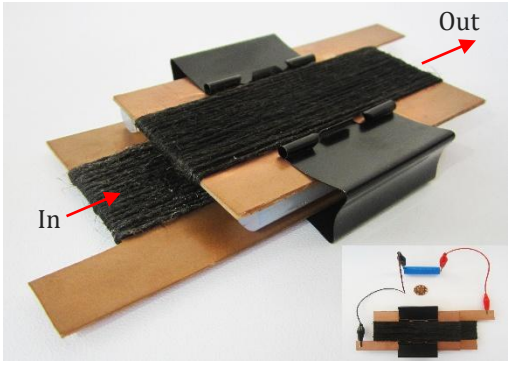

Figure 3: Final functional prototype

To form the functional prototype, two such identical CA thread electrodes were arranged in a parallel plate geometry and two polypropylene bar (2.5 Inch × 0.5 Inch × 0.25 Inch) used as a spacer to provide space between two edges by creating a channel for the flow of the feedstock solution and reducing the fouling risk. In the experimental CDI setup, the flow of the contaminated feedstock solution was either carried out through the gravitational force when the functional device was kept at an angle of 25° or using a peristaltic pump with a flow rate of 25 mL/min.

2.4. Electrosorption Experiments & Performance Evaluation

To operate the device, 1.2 V applied potential was supplied by a typical single pen-torch (AA) battery to avoid water hydrolysis at 1.23 V (Fan, Tseng, Li, & Hou, 2016). In order to investigate the

effectiveness of the functional device with the commercial system, the same effluent solution was passed through the functional device consist of 10 g of CAs thread (25 wt.% of AEM per sample) and the traditional CE-2 RO system (operating voltage, 220 V) under the same experimental conditions. A total of 12 consecutive rounds of single-pass filtration were carried out through the functional device consist of 10 g of PCA thread (25 wt.% of AEM per sample) electrode for each pollutant by without applying any voltage and with applying 1.2 V to evaluate the effect of applying voltage on the sorption capacity of the functional prototype. The electrosorption experiments were repeated for several times to confirm the reproducibility of the experiments and the remaining NaCl and As ($^{5+}$) effluent solution was analyzed.

2.4.1. *Determining the Synthetic NaCl Removal Capacity of CAs Thread Electrode*

To evaluate the desalination performance of CAs thread electrode in synthetic concentration, 50 ml of each DIW solution containing 50 ppm to 2000 ppm of NaCl salt was used as a saline feedstock. The change in the conductivity of NaCl solution was monitored using the HI2030 edge EC/TDS/Salinity meter with the HI763100 four ring platinum conductivity probe then the conductivity values were converted to ppm format. The saline removal capacity of the CAs thread electrode was calculated according to the following equation (Alagappan, Heimann, Morrow, Andreoli, & Barron, 2017):

$$Filtration\ Capacity\ (\%) = [1- \frac{C_t}{C_0}] \times 100 \quad \text{..... (1)}$$

Where C_t and C_0 indicate the concentration of the filtered solution and initial concentration respectively.

2.4.2. Determining the Effectiveness of CAs Thread Electrode in filtering Synthetic Arsenic ($^{5+}$) ions

To investigate the heavy metal filtering capabilities of CAs thread electrode device, 50 ml of each DIW solution containing 50 to 2000 ppm of arsenic pentoxide was used as a heavy metal feedstock solution. The change in the arsenic concentration was measured using Inductively Coupled Plasma-Optical Emission Spectrometer (ICP-OES) and calculated according to the equation (1).

2.5. Characterization Experiments

Nitrogen adsorption-desorption isotherms were obtained by a nitrogen adsorption apparatus (ASAP-2010, USA) after outgassing the samples for 6 hours at 280 °C under high vacuum for characterizing the synthesized CAs. The specific surface area and average pore diameter of the synthesized CAs were calculated using the Brunauer-Emmett-Teller (BET) method. The Raman

spectra were obtained using a confocal Raman microscope (MonoVista CRS+, S&I GmbH) with 532 nm wavelength incident laser light and the surface morphology of the CAs and CAs thread were characterized by field emission scanning electron microscopy (JSM-7610F, JEOL Ltd.). The atomic percentage analysis of CAs was conducted by Energy-dispersive X-ray spectroscopy (Instrument, 7610F). The static contact angle with water was measured by a JY-PHb Contact angle measurement.

2.6. Electrochemical Measurements

The cycle voltammetry measurements (CHI660E, electrochemical work-station) of the CAs thread were performed by three electrodes test system at room temperature to evaluate its electrochemical performance while the galvanostatic charge-discharge measurement (GCD, Huakeputian Technology Co., Ltd., Beijing, China) was carried out with a two-electrode arrangement. The mass of the active material of each electrode was about 4.25 mg. The specific capacitance (C_{sp} in F g^{-1}) can be calculated from the GCD curve according to the following equation (Cai, Tan, Deng, Liu, & Gui, 2019):

$$C_{sp} = \frac{I\Delta t}{\Delta V \times m} \quad \text{...} \quad (2)$$

Where I is the constant discharge current (A), Δt is the discharge time (s), ΔV is the working voltage window and m is the mass of the active material of each electrode.

3. RESULTS & DISCUSSION

3.1. The N_2 Adsorption-Desorption Isotherms & Pore Size Distribution Curves

Figure 4 and 5, shows N_2 adsorption-desorption isotherms and pore-size distribution curves of PCA and MCA. According to the analyzed data of adsorption characteristics, the specific surface area was 1785 m^2/g and 1471 m^2/g for PCA (Fig. 4 (a)) and MCA (Fig. 5 (a)) respectively. Such a high specific surface area could be attributed to the pores, including micropores (< 2 nm) and mesopores (2-50 nm), resulted by the interval gaps between chains of interconnected nanoparticles and this high specific surface area is beneficial to achieve higher electrosorption capacity (Zhu, et al., 2017; Zhu, et al., 2016).

There is a broad distribution within the detectable range of pore sizes (0.7-38 nm) for PCA samples (Fig. 4 (b)) and the average pore diameter of all the PCA samples was within the range of microporosity. The average pore size of the PCA sample is 1.7 nm. However, in the detectable range of pore sizes (1.0-40.0 nm), the pore structure of MCA (Fig. 5 (b)) is mesoporous with the average pore

size is 2.3 nm~2.5 nm. Mesoporosity has reached over 70% in the MCA samples. This excellent pore size distribution and opened network structure of PCA and MCA would endow the ultra-low-density CAs with excellent electrochemical performance.

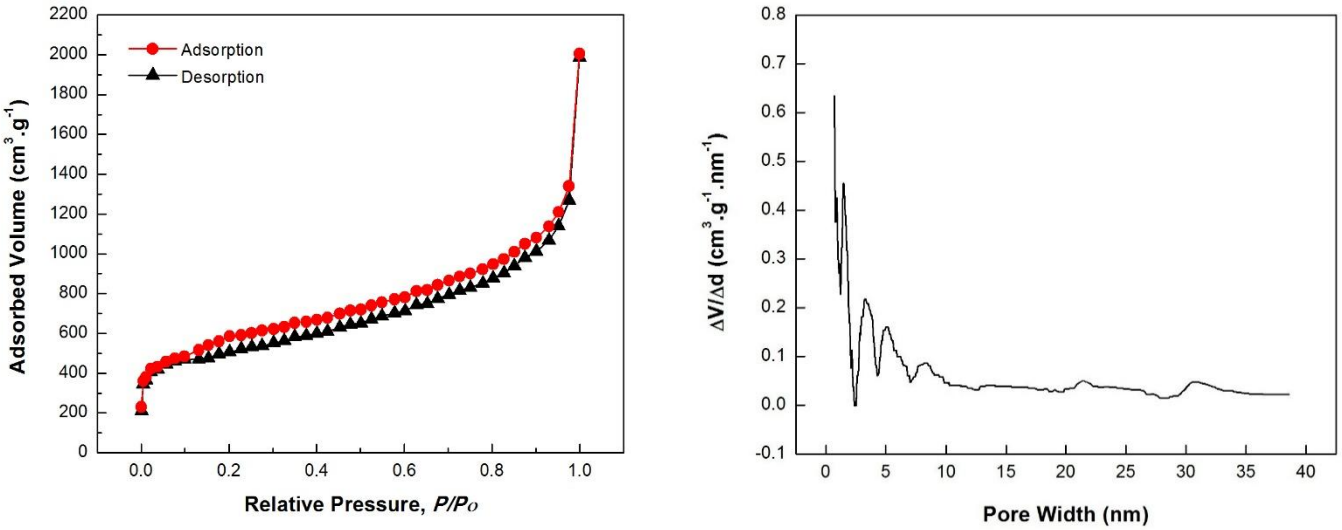

(a) **(b)**

Figure 4: (a) N_2 adsorption-desorption isotherms (b) and pore-size distribution curves of PCA samples

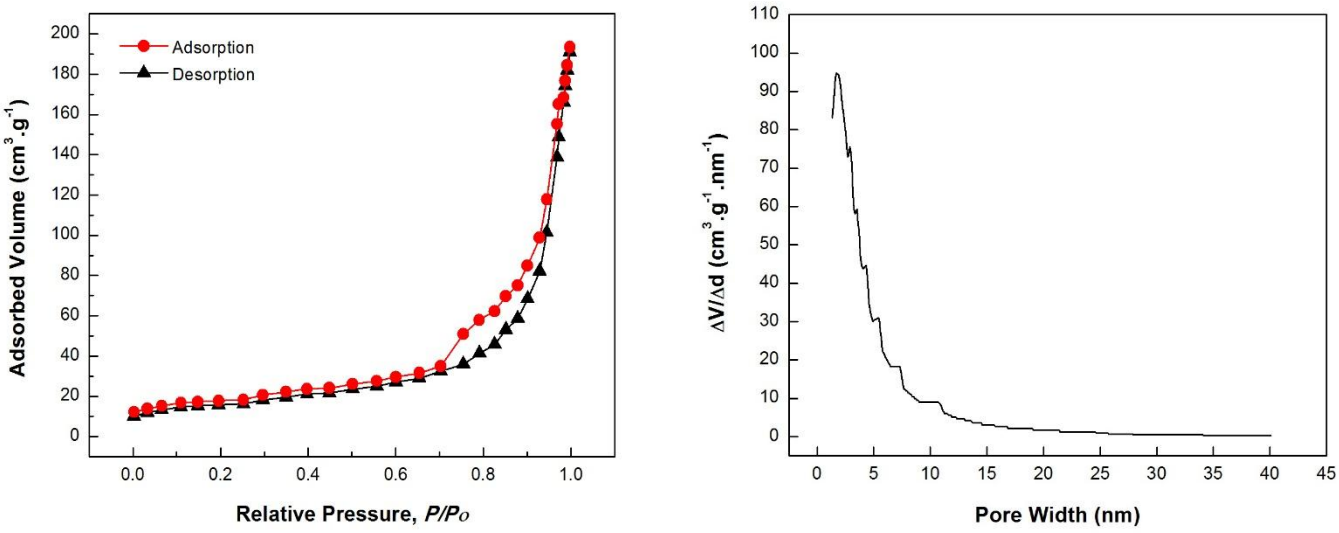

(a) **(b)**

Figure 5: (a) N_2 adsorption-desorption isotherms (b) and pore-size distribution curves of MCA samples

3.2. Analysis of Raman Spectroscopy

The Raman spectrum of CAs is characterized by two main features including the *G* mode and the *D* mode. The *G* band is associated with the in-plane vibrations of sp^2 bonded carbon atoms,

corresponding to the C-C stretching in the graphitic lattice (Zhu, et al., 2016). While the *D* band corresponds to unordered carbon or defective graphitic structures (Zhai, et al., 2017).

The Raman spectrum of synthesized PCA samples (Fig.6 (a)) displays two strong bands at 1372.310 cm^{-1} (*D* band) and 1607.601 cm^{-1} (*G* band) where these bands are the major characteristics of CAs structure (Zhu, et al., 2017; Zhu, et al., 2016). Similarly, MCA samples (Fig.6 (b)) also exhibits two sharp peaks at 1335.264 cm^{-1} (*D* band) and 1591.126 cm^{-1} (*G* band) which are the corresponding characteristic feature of CAs framework (Zhai, et al., 2017). The intensity of the *G* band for both samples was stronger than the intensity of the *D* band in this study, indicating that the disorder or defects of the carbon-based lattice were negligible (Zhu, et al., 2017).

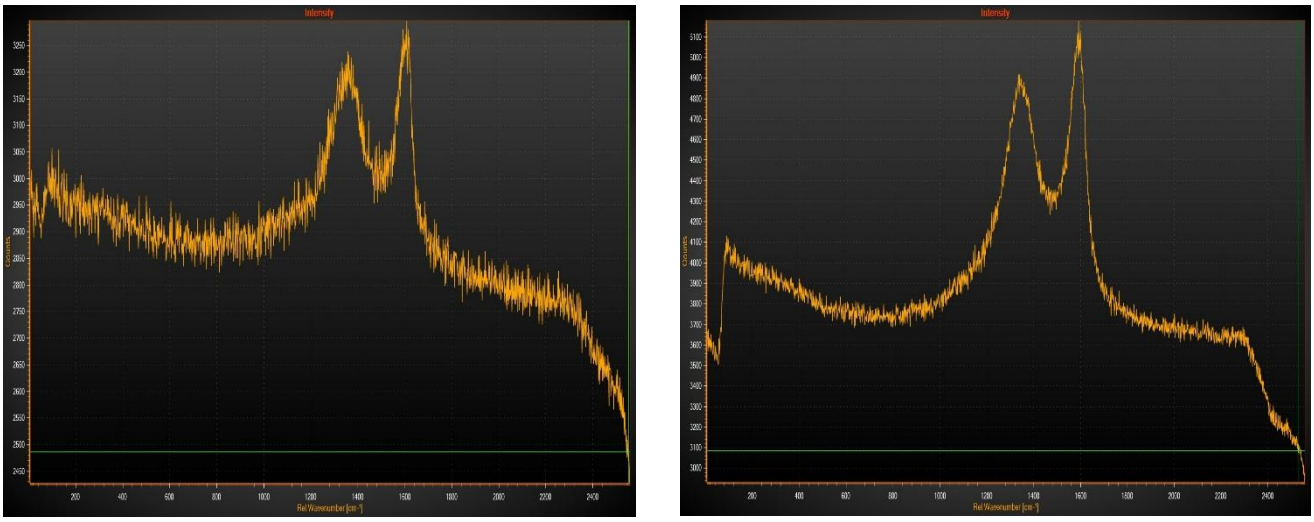

(a) **(b)**

Figure 6: Raman spectrum (532 nm laser excitation wavelength) of (a) PCA samples (b) and MCA samples

3.3. Field Emission Scanning Electron Microscopy (FE-SEM) Images

The FE-SEM images of non-treated raw PET sample (Fig. 7 (a)) demonstrates that its surface is smooth, plane and uniform. However, the PCA (Fig. 7 (b)) and MCA (Fig. 7 (c)) samples confirm a non-uniform porous structure with multiple pore types ranging from micropores to mesoporous and highly cross-linked interconnected three-dimensional networks at higher magnification of 1 µm.

The FE-SEM images of PCA thread (Fig. 7 (e)) and MCA thread (Fig. 7 (f)) shows that the surface structure of CAs thread is relatively uneven, cracked and irregular than pristine jute thread (Fig. 7 (d)) at 10 µm magnification which revealed that the nanoporous CAs were deposited on the jute thread matrix successfully.

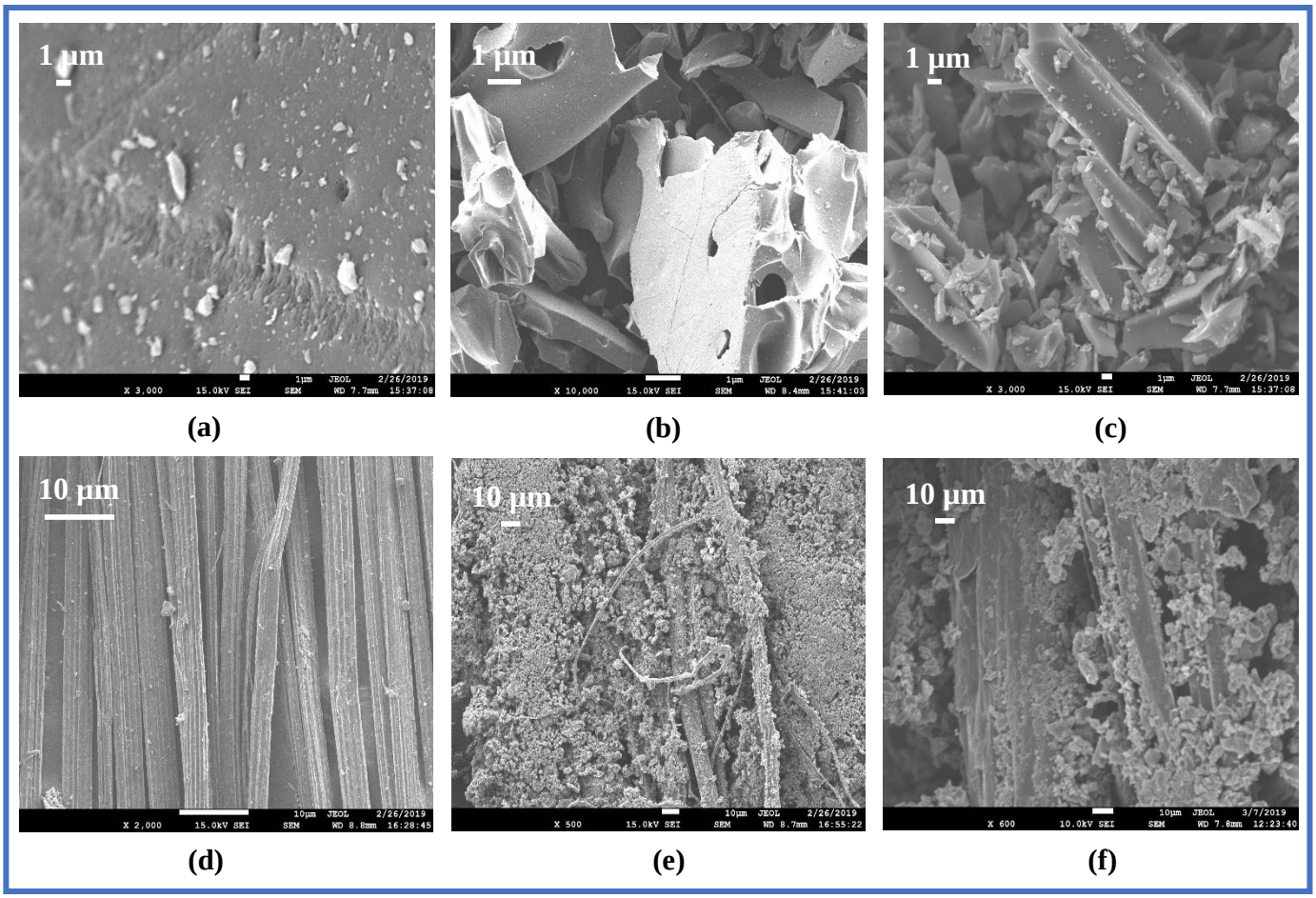

Figure 7: FE-SEM image of (a) non-treated PET plastic surface, (b) PCA samples, (c) MCA samples, (d) pristine jute thread, (e) PCA thread, (f) and MCA thread

3.4. Analysis of Energy-dispersive X-ray spectroscopy (EDX)

The chemical characterization of synthesized PCA (Fig. 8 (a)) and MCA (Fig. (8b)) samples were conducted using the EDX technique. The EDX spectra of PCA samples revealed that the CAs synthesized from only PET waste, contains relatively higher Carbon (C) content than CAs synthesized from mixed plastic waste. In contrast, PCA samples contain relatively lower Oxygen (O) functionalities than MCA samples with almost no residual carbonaceous impurities.

However, metal impurities such as Iron (Fe) or Aluminum (Al) were detected in the atomic arrangement of CAs synthesized from the mixed plastic waste which requires additional purification stages to get the pure CAs (Karaaslan, Kadla, & Ko, 2016). The presence of metallic quantities and higher carbonaceous impurities of MCA samples suggested that CAs synthesized from PET waste will be a more effective and feasible strategy instead of mixed plastic waste for synthesizing CAs.

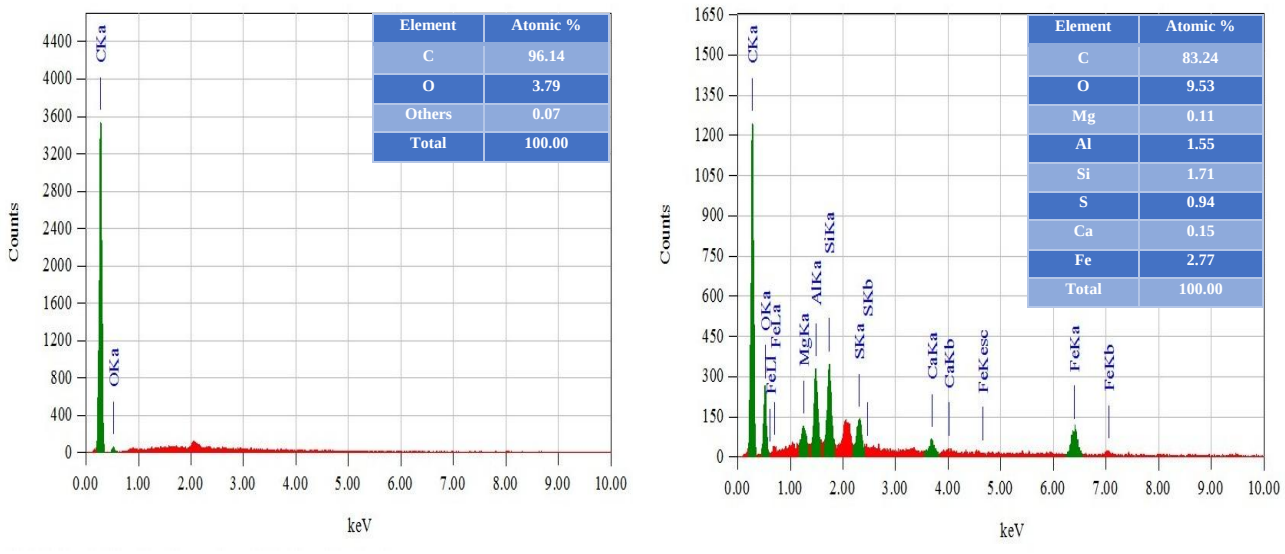

(a) **(b)**

Figure 8: EDX spectra of CAs synthesized from (a) PET waste (b) and mixed plastic waste

3.5. Electrochemical Characterizations & Contact Angle Measurement

3.5.1. Analysis of Cycle Voltammetry (CV) Curves

The CV curves of PCA thread (Fig. 9 (a)) and MCA thread (Fig. 9 (b)) at different scan rates (50-100 mV s^{-1}) exhibit symmetric and a near-ideal rectangular shape without any redox peak which illustrates the rapid formation of EDL without any Faradaic reaction and the electrical resistance is negligible (Cai, Tan, Deng, Liu, & Gui, 2019; Hou, Huang, & Hu, 2013). This electrochemical behaviour confirms the role of copper (Cu) sheet in a functional device for providing an equipotential surface without any direct involvement in the water purification stages and due to the non-faradic process, no additional chemical reaction occurred in the electrode surface during the filtration experiments (Moronshing & Subramaniam, 2017). The retention of the shape and structure of the CV curves for both PCA thread and MCA thread at higher scan rates (100 mV s^{-1}) confirms the rapid formation of EDL with the absence of pseudo-capacitance and a good rate capability which is the best explanation for understanding the functional devices excellent electrochemical performance and the high electrosorption capacity (Cai, Tan, Deng, Liu, & Gui, 2019; Hou, Huang, & Hu, 2013).

3.5.2. Analysis of Galvanostatic Charge-Discharge (GCD) Curves

The GCD curves of PCA thread and MCA thread in Figure 10 (a) displays an almost symmetric triangular shape and rapid responses of current-voltage. It is elucidating an ideal capacitive behaviour of the device with excellent electrochemical reversibility (Cai, Tan, Deng, Liu, & Gui, 2019). The PCA

thread exhibits relatively high specific capacitance and the longest charge-discharge time than MCA thread without any significant ohmic drop. The specific capacitance of PCA thread and MCA thread were calculated according to equation (2) which is 173 F g^{-1} and 125 F g^{-1} respectively at a current density of 0.5 A g^{-1}.

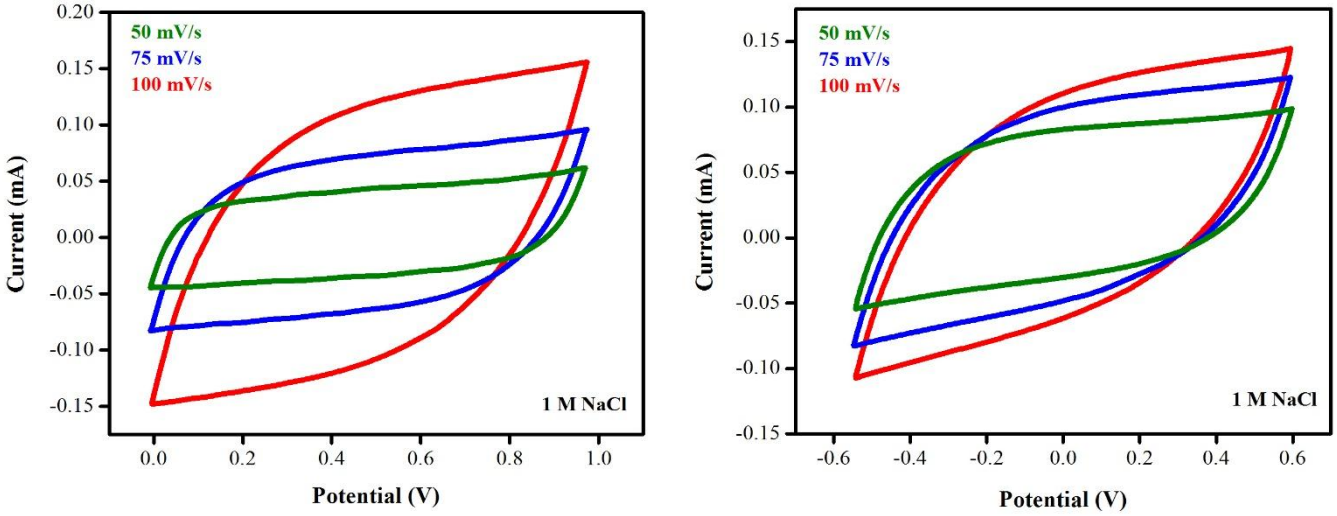

Figure 9: (a) CV curves of PCA thread and (b) MCA thread at 1 M NaCl (electrolyte) concentrations of feedstock solutions.

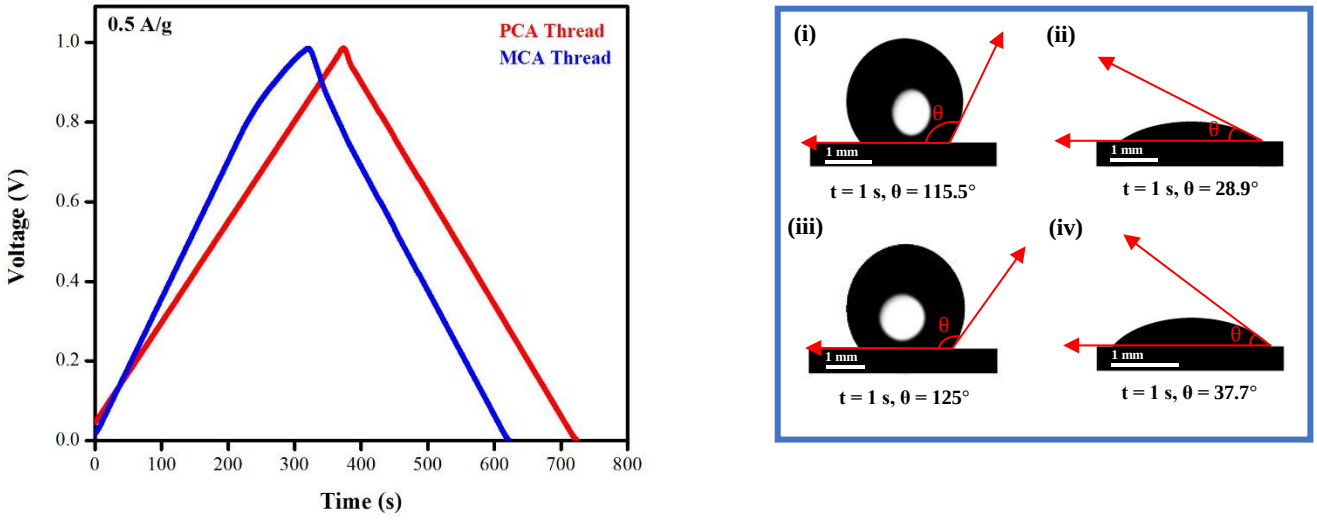

Figure 10: (a) GCD curves of CAs thread at a current density of 0.5 A g^{-1} and (b) contact angle measurements of (i) PCA sample, (ii) PCA thread, (iii) MCA sample & (iv) MCA thread.

3.5.3. Analysis of Contact Angle Measurement

The contact angle between the feedstock and the electrode surface is an important parameter for

achieving the higher water filtration efficiency in CDI technique (Moronshing & Subramaniam, 2017). Figure 10 (b) illustrating the initial contact angle of 115.5° and 125° of synthesized pure PCA and MCA samples respectively which are confirming their hydrophobic nature. However, the contact angle of PCA and MCA samples were reduced to 28.9° and 37.7° respectively when the samples were immobilized on a jute thread surface and thus the CAs thread is inherently more hydrophilic than the pure CAs samples. The presence of naturally abundant cellulose matrix in the biocompatible jute thread surface predominantly contributes to the increased hydrophilicity of the CAs thread electrodes.

3.6. Filtration Experiments, Performance Evaluation & Water Purification Mechanism

Figure 11 demonstrates that the functional device consists of the PCA thread sample exhibits a relatively higher filtration capacity than MCA thread sample by removing nearly 100% of both cationic (Na^+, As^{5+}) and anionic (Cl^-) contaminants from the feedstock solution at the concentration range of $\leq$1000 ppm where the commercial RO system was proven ineffective. The key principle of conventional semi-permeable RO filtration system is separating the bulk water instead of separating specific ionic contaminants from the feedstock solution which could be the possible reason behind the less filtration effectiveness comparing with CDI based CAs thread electrodes at the concentration range of $\leq$1000 ppm (Kim, Gorski, & Logan, 2017). In contrast, the CAs thread electrode in this study predominately extracts the positively and negatively charged contaminants ions from water to migrate towards the porous CAs surface and to be adsorbed into the EDL. However, the commercial RO system shows relatively higher average filtration efficiency than MCA thread electrode at the concentration range of >1000 ppm where the PCA thread electrode still exhibits exceptionally high overall filtration efficiency of above 90%.

Contaminant		**Overall Filtration Capacity (%)**		
		PCA thread (1.2 V)	**MCA thread (1.2 V)**	**RO (220 V)**
NaCl	Concentration (50-1000 ppm)	**99.73**	91.78	**75.51**
	Concentration (1050-2000 ppm)	**92.77**	73.89	**99.91**
As ($^{5+}$)	Concentration (50-1000 ppm)	**99.79**	95.29	**83.43**
	Concentration (1050- 2000 ppm)	**95.21**	87.37	**99.97**

Figure 11: Comparison of overall NaCl and As ($^{5+}$) removal capabilities at a different concentration between CAs thread electrode and conventional RO filtration system under the same conditions

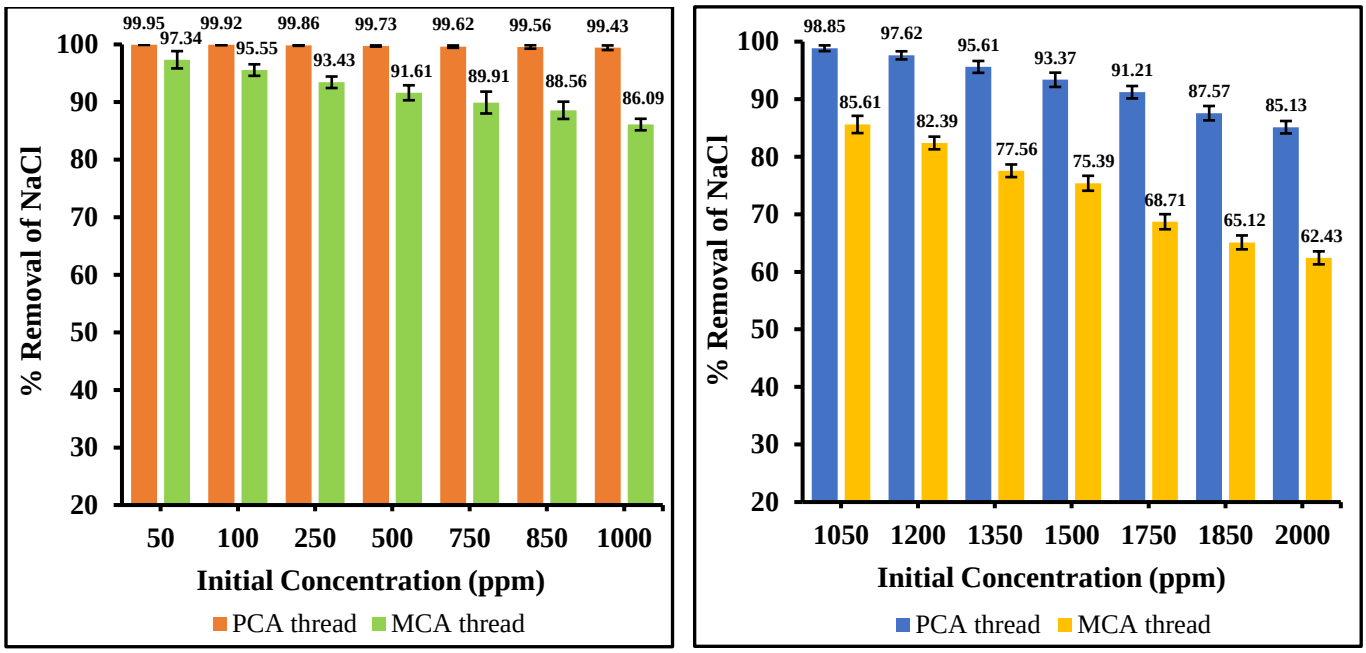

(a) **(b)**

Figure 12: NaCl filtration capabilities of per 10 g of CAs thread (25 wt.% of AEM per sample) in the functional device assembly by applying 1.2 V at the concentration range of (a) 50-1000 ppm and (b) 1050-2000 ppm through the consecutive single-pass filtrations experiments, that took on average, 120 s to filter 50 ml of each NaCl solution

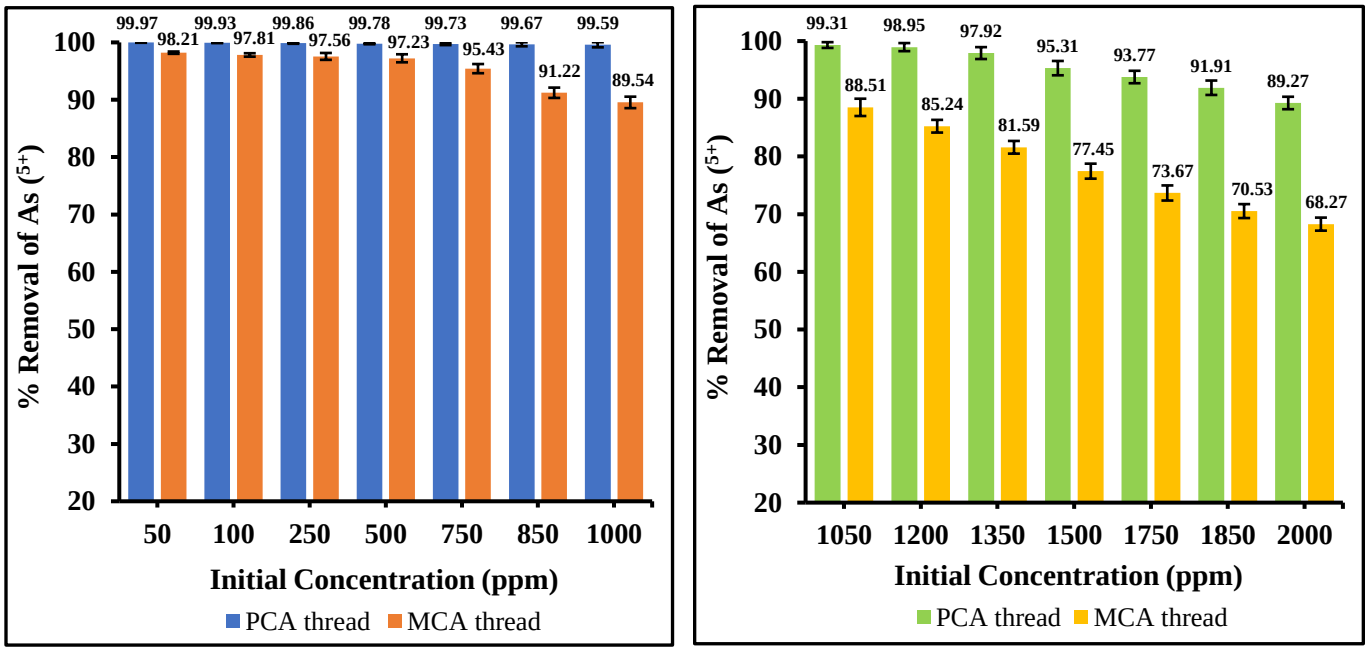

(a) **(b)**

Figure 13: As ($^{5+}$) filtration capabilities of per 10 g of CAs thread (25 wt.% of AEM per sample) in the functional device assembly by applying 1.2 V at the concentration range of (a) 50-1000 ppm and (b) 1050-2000 ppm through the consecutive single-pass filtrations experiments, that took on average, 120 s to filter 50 ml of each As ($^{5+}$) solution

Figure 12-13 demonstrated the detailed filtration study of CAs thread electrodes ranging from intermediate feedstock concentration range of 50-1000 ppm to high concentration range of 1050-2000 ppm. PCA thread electrode demonstrates comparatively higher filtration capabilities than MCA thread electrode through the single-pass experiments for eliminating both cationic (Na^{+}, As^{5+}) and anionic (Cl^{-}) contaminants from feedstock solution without generating any secondary pollution. High specific surface area (1785 m^2/g) of PCA samples, high specific capacitance (173 F g^{-1}) and low hydrophobicity (28.9°) of PCA threads are predominately contributed during the filtration experiments and these parameters are the possible key factors to understand the superior high filtration phenomenon of PCA thread electrode.

Additional experiments were conducted through without applying any voltage and with applying 1.2 V to investigate the effects of applied voltage on the adsorption performance of PCA thread electrode. 1.2 V was chosen as ideal voltage criteria because when the potential difference across the 1.23 V in CDI setup, the bond between the hydrogen and the oxygen atoms breaks which leads to the electrolysis reaction of water (Fan, Tseng, Li, & Hou, 2016). Figure 14 demonstrates that without applying any voltage the PCA thread electrode was still capable of removing salt and heavy metal contaminants from the feedstock solution and the breakthrough were observed after applying an additional voltage of 1.2 V. The concentration of arsenic (As^{5+}) ions in residual solution were all below

Filtration Trial	**Residual NaCl Concentration (ppm)**		**Residual As ($^{5+}$) Concentration (ppm)**	
	0.0 V	**1.2 V**	**0.0 V**	**1.2 V**
1	16.73	**N.D.**	16.67	**N.D.**
2	16.93	**N.D.**	16.73	**N.D.**
3	17.53	**N.D.**	16.78	**N.D.**
4	17.71	**N.D.**	16.87	**N.D.**
5	17.77	**N.D.**	16.93	**N.D.**
6	17.91	**1.13×10^{-3}**	17.11	**N.D.**
7	18.13	**1.27×10^{-3}**	17.23	**N.D.**
8	18.29	**1.33×10^{-3}**	17.43	**N.D.**
9	18.33	**1.51×10^{-3}**	17.53	**1.11×10^{-3}**
10	18.57	**1.55×10^{-3}**	17.61	**1.26×10^{-3}**
11	18.73	**1.67×10^{-3}**	17.73	**1.35×10^{-3}**
12	18.89	**1.71×10^{-3}**	17.93	**1.42×10^{-3}**

N.D.: Not Detected

Figure 14: Filtration capabilities of PCA thread electrodes with different operating voltage through 12 consecutive single-pass filtrations trials, 50 ml at a time, of 25 ppm of contaminated feedstock solution

the World Health Organization (WHO) guideline value of 10 µg/L (10×10^{-3} ppm) and Bangladesh permissible limit of 50 µg/L (50×10^{-3} ppm). The high filtration capabilities of PCA thread electrode is attributed to the electrostatic attraction at 1.2 V whereas adsorption at 0.0 V is due to the specific adsorption and physisorption (Fan, Tseng, Li, & Hou, 2016).

The applied potential difference generates an electric field where the positive ions (Na^+, As^{5+}) and negative ions (Cl^-) are electrostatically adsorbed onto the microporous or mesoporous counter-electrode surface via electrostatic interactions and an EDL is formed at the electrode-solution interface (Fan, Tseng, Li, & Hou, 2016) which is illustrated in figure 15. Typically, after long hours of adsorption-desorption cycles, the electrode becomes saturated in contaminants ions then it can be easily regenerated for the next adsorption cycle by electrical discharge or removing the applied electric potential to release the adsorbed ions back to a waste concentrate stream (Gao, Omosebi, Landon, & Liu, 2015).

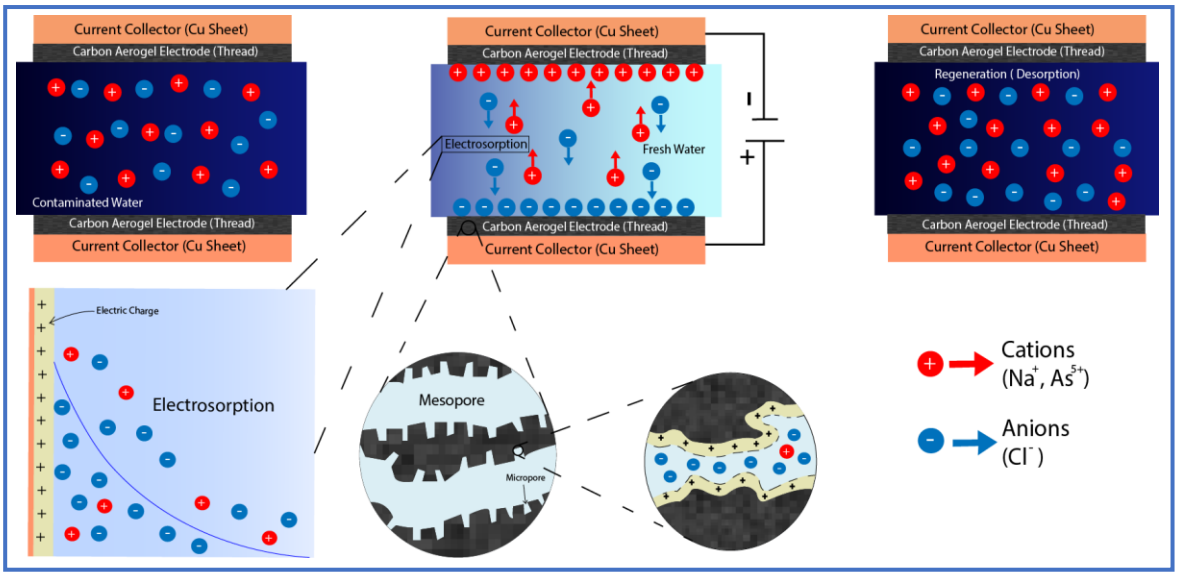

Figure 15: NaCl and Arsenic electrosorption mechanism of CAs thread electrode

4. CONCLUSIONS & FUTURE WORK

A novel, non-invasive and chemical-free strategy was developed in this study for fabricating highly porous CAs from thermoplastic waste through overcoming the synthesizing route drawbacks of the existing sol-gel method via addressing a sustainable route for minimizing the thermoplastic pollution. The synthesized CAs were immobilized on a locally available, biocompatible and flexible jute thread substrate in a simple and scalable pathway for an effective electrode-water interface. The single-pass filtration experiments conducted at 1.2 V demonstrated that the PCA thread electrode is super-effective at the intermediate concentration range of $\leq$1000 ppm where the commercial RO system was proven ineffective. Additionally, the PCA thread electrode still exhibits remarkably high

overall filtration efficiency of above 90% at the high feedstock concentration range of >1000 ppm.

In future, further study could be conducted to investigate the feasibility of the functional device for inactivating the cell wall of various types of pathogenic bacteria that carries an electrical charge in the contaminated concentrations such as *E. coli* or one possible extension could be experimenting with other water pollutants such as As^{3+} or Cr^{6+} to evaluate the effectiveness of the functional device. The functional device can be adopted in both industrial and domestic settings by ensuring the growing demand for on-spot water remediation by expanding the market to include consumer use.

The simple assembly of the functional device demonstrated its capability to operate using only gravitational water flow by eliminating the requirement of any special water pumping system with minimal fouling risk. From an energy consumption perspective, a low voltage of 1.2 V is sufficient to operate the device which could be easily supplied by using photovoltaics or any renewable power resources. The high-performance efficiency with portable adaptability, scalability of the entire process and minimal energy consumption which attributed to the low investment and infrastructure cost, make the functional device suitable for practically employing in the under-developed communities of geographically remote areas who do not have access to a centralized water supply.

5. REFERENCES

Alagappan, P. N., Heimann, J., Morrow, L., Andreoli, E., & Barron, A. R. (2017). Easily Regenerated Readily Deployable Absorbent for Heavy Metal Removal from Contaminated Water. *Nature, Scientific Reports*, 1-7. doi:10.1038/s41598-017-06734-7

Araby, S., Qiu, A., Wang, R., Zhao, Z., Wang, C.-H., & Ma, a. J. (2016). Aerogels based on carbon nanomaterials. *J Mater Sci, Springer*. doi:10.1007/s10853-016-0141-z

Bi, H., Yin, Z., Cao, X., Xie, X., Tan, C., Huang, X., . . . Zhang, a. H. (2013). Carbon Fiber Aerogel Made from Raw Cotton: A Novel, Efficient and Recyclable Sorbent for Oils and Organic Solvents. *Advanced Materials*, 5916–5921. doi:10.1002/adma.201302435

Cai, X., Tan, G., Deng, Z., Liu, J., & Gui, D. (2019). Preparation of Hierarchical Porous Carbon Aerogels by Microwave Assisted Sol-Gel Process for Supercapacitors. *Polymers*, 1-11. doi:10.3390/polym11030429

Chandrasekaran, S., Campbell, P. G., Baumann, T. F., & Worsleya, a. M. (2017). Carbon aerogel evolution: Allotrope, graphene-inspired, and 3D-printed aerogels. *INVITED REVIEW*, 1-20. doi:10.1557/jmr.2017.411

Fan, C.-S., Tseng, S.-C., Li, K.-C., & Hou, C.-H. (2016). Electro-Removal of Arsenic(III) and Arsenic(V) from Aqueous Solutions by Capacitive Deionization. *Journal of Hazardous Materials*. doi:10.1016/j.jhazmat.2016.03.055

Farmer, J., Richardson, J., Fix, D., Thomson, S., & May, S. (1996). *Desalination with Carbon Aerogel Electrodes.* Livermore, California: Lawrence Livermore National Laboratory.

Gao, X., Omosebi, A., Landon, J., & Liu, K. (2015). Enhanced Salt Removal in an Inverted Capacitive Deionization Cell Using Amine Modified Microporous Carbon Cathodes. *Environmental Science & Technology*, 10920−10926. doi:10.1021/acs.est.5b02320

Herou, S., Schlee, P., Jorge, A. B., & Titirici, M. (2018). Biomass-derived electrodes for flexible supercapacitors. *Current Opinion in Green and Sustainable Chemistry*, 18-24. doi:10.1016/j.cogsc.2017.10.005

Hou, C. H., Huang, C. Y., & Hu, C. Y. (2013). Application of capacitive deionization technology to the removal of sodium chloride from aqueous solutions. *Int. J. Environ. Sci. Technol.*, 753–760. doi:10.1007/s13762-013-0232-1

Hu, P., Tan, B., & Long, a. M. (2016). Advanced nanoarchitectures of carbon aerogels for multifunctional environmental applications. *Nanotechnology Review*, 23–39. doi:10.1515/ntrev-2015-0050

Jagdale, P., Sharon, M., Kalita, G., Maldar, N. M., & Sharon, M. (2012). Carbon Nano Material Synthesis from Polyethylene by Chemical Vapour Deposition. *Advances in Materials Physics and Chemistry*, 1-10. doi:10.4236/ampc.2012.21001

Jahan, H. (2016). Arsenic in Bangladesh: how to protect 20 million from the world's largest poisoning. *The Guardian*. Retrieved from https://www.theguardian.com/global-development-professionals-network/2016/oct/18/arsenic-contamination-poisoning-bangladesh-solutions

Jia, B., & Zhang, W. (2016). Preparation and Application of Electrodes in Capacitive Deionization (CDI): a State-of-Art Review. *Nanoscale Research Letters*, 1-25. doi:10.1186/s11671-016-1284-1

Karaaslan, M. A., Kadla, J. F., & Ko, a. F. (2016). *Lignin in Polymer Composites.* Elsevier Inc. doi:10.1016/B978-0-323-35565-0.00005-9

Kim, T., Gorski, C. A., & Logan, B. E. (2017). Low Energy Desalination Using Battery Electrode Deionization. *Environmental Science & Technology Letters*, 444−449. doi:10.1021/acs.estlett.7b00392

M.F.Hossain. (2019). Arsenic contamination in Bangladesh-An overview. *Agriculture, Ecosystems & Environment*, 1-16. doi:10.1016/j.agee.2005.08.034

Mahmud, I. (2018). Bangladesh pours fifth largest chunk of plastic into sea. *Prothom Alo Environment*. Retrieved from https://en.prothomalo.com/environment/news/177094/73-thousand-tonnes-of-plastic-waste-enters-the-sea

Molla, M. A.-M. (2018). Plastic chokes Dhaka's drainage. *The Third Pole*. Retrieved from https://www.thethirdpole.net/en/2018/04/09/plastic-chokes-dhakas-drainage/

Moronshing, M., & Subramaniam, C. (2017). Scalable Approach to Highly Efficient and Rapid Capacitive Deionization with CNT-Thread As Electrodes. *ACS Applied Materials & Interfaces*, 39907−39915. doi:10.1021/acsami.7b11866

Rabbani, G., Munira, S., & Saif, S. (2018). Coastal Community Adaptation to Climate Change-Induced Salinity Intrusion in Bangladesh. *Coastal and Marine Environments - Physical Process, IntechOpen*, 1-13. doi:10.5772/intechopen.80418

Sarker, M., Kabir, A., Rashid, M. M., Molla, M., & Mohammad, a. A. (2011). Waste Polyethylene Terephthalate (PETE-1) Conversion into Liquid Fuel. *Journal of Fundamentals of Renewable Energy and Applications*, 1-5. doi:10.4303/jfrea/R101202

Xu, P., Drewes, J. E., Heil, D., & Wang, G. (2008). Treatment of brackish produced water using carbon aerogel-based capacitive deionization technology. *WATER RESEARCH*, 2605-2617. doi:10.1016/j.watres.2008.01.011

Zhai, Z., Wang, S., Xu, Y., Zhang, L., Yan, M., & Liu, Z. (2017). Carbon aerogels with modified pore structures as electrode materials for supercapacitors. *J Solid State Electrochem*, 1-11. doi:10.1007/s10008-017-3699-8

Zhang, Z., Feng, J., Jiang, Y., & Feng, a. J. (2018). Hierarchically porous carbon aerogels with high specific surface area prepared from ionic liquids via salt templating method. *Carbon Letters*, 47-54. doi:10.5714/CL.2018.28.047

Zhu, J.-y., Yang, X., Fu, Z.-b., Wang, C., Wu, W.-d., & Zhang, L. (2016). Fabrication of ultra-low density, high surface area carbon aerogels and their application in supercapacitors. *Materials Science Forum*, 1349-1355. doi:10.4028/www.scientific.net/MSF.852.1349

Zhu, L., Wang, Y., Wang, Y., You, L., Shen, X., & Li, S. (2017). An environmentally friendly carbon aerogels derived from waste pomelo peels for the removal of organic pollutants/oils. *Microporous and Mesoporous Materials*, 1-20. doi:10.1016/j.micromeso.2016.12.033